Detailed shape modeling of a local topography using thermal infrared imager data and evaluation of thermal inertia of asteroid 162173 Ryugu

M. Ito[1] , S. Tanaka[2], N. Sakatani[3] , H. Senshu[4]
[1]The University of Tokyo, [2]Institute of Space and Astronautical Science, [3]Rikkyo University, [4]Chiba Institute of Technology

Introduction: Hayabusa2 is equipped with a Thermal Infrared Imager (TIR) to observe surface temperature of the asteroid Ryugu. The results of the TIR observations indicated that the global thermal inertia of Ryugu is 225 ± 45 [J m^{-2} K^{-1} $s^{-0.5}$, hereafter tiu][1] in spite of its rocky surface, while such large boulders on earth commonly have higher inertia value as 1000-2000 tiu. In general, fine-grained soils or rocks with higher porosity show larger diurnal surface temperature variation than that of dense rocks. The results of the global thermal behavior were analyzed by temperature variations of TIR images with a resolution of about 5 m. The estimated low thermal inertia may be caused by the original nature of high porous boulders and/or fine dust covering with dense boulders. High resolution and thermophysical structure including depth dependency is important to reveal the characteristics of the thermal structure of Ryugu and the origin of its formation. In this study, we analyzed the surface temperature distribution in the detailed topography of asteroid Ryugu using high-resolution (27 cm/pix or less) TIR images taken at altitudes lower than 300 m.

Method: By solving the following one dimensional heat conduction equation and boundary conditions for the asteroid surface, we can obtain the temperature variation of the surface of Ryugu with solar radiation;

$$\frac{\partial T}{\partial t} = \frac{k}{\rho c}\frac{\partial^2 T}{\partial z} \quad (1)$$

$$(1-A)F_s(t) = -k\frac{\partial T}{\partial z}|_{z=0} + \epsilon\sigma T_{z=0}^4 \quad (2)$$

$$\frac{\partial T}{\partial z}|_{z=z_0} = 0 \quad (3)$$

T[K]: temperature, t[s]: difference time, k [J m^{-1} K^{-1} s^{-1}]: thermal conductivity, ρ [kg m^{-3}]: density, c [J kg^{-1} K^{-1}]: specific heat, z [m]: difference distance, A [-]: bond albedo, F_s[W m^{-2}]: solar input, ϵ[-]: emissivity, σ[W m^{-2} K^{-4}]: Stefan-Boltzmann constant, respectively. The thermal simulation code, which is taken into account of both local topography and secondary radiation effect developed by Takita et al., (2017) was used in this study.

In contrast to the global thermal analysis[1], the observational conditions such as insolation angle, emission angle, and so on, of close up images at the low altitude are limited. Since the incident energy also varies with local slope of the terrain, a detailed topographic model is required for accurate estimation of the thermal behavior to compare with the high resolution images. In the close up TIR images, shadowed area formed by adjacent large boulders or by local inclination of the terrain can be observed. Using precise thermal simulation, we can evaluate thermal inertia of these shaded area at the same time. These area just before sun exposure might reflect on deeper part of thermal inertia, for example, the skin depth is 4.4 cm when the duration of shadow is equivalent to that of one rotation period of 7.6 h (thermal diffusivity is assumed to be 6.3×10^{-8} [m^2 s^{-1}] which is comparable to 225 tiu of global averaged value of thermal inertia). On the contrary, the rapid temperature increase by abrupt insolation from the shadowed area should be attributed to the uppermost thermal properties. Therefore, it is possible to evaluate depth dependency of the thermal inertia by close up image analysis.

In this study, we selected the region around the second touchdown site at where a large number of close up TIR images were taken. We constructed a local terrain model by Shape-from-Motion method (SfM) using more than 150 high-resolution (27 cm/pix or less) TIR images taken at altitudes lower than 300 m. Using this local terrain model, we performed thermal simulation assuming a uniform thermal inertia from 150 to 800 tiu. To be able to compare the simulation results with the TIR images, image matching was applied for the simulation result using a projection transformation technique. Then, a distribution map of thermal inertia at the target area was produced by comparing the temperature data pixel by pixel.

Result and discussion: Using 158 high-resolution (27 cm/pix or less) TIR images taken near the second touchdown point, we constructed an accurate local terrain model with a resolution of 9.77 cm (Fig. 1). Using the red area in Fig. 1, a thermal simulation was performed to obtain Fig. 2(a). In this figure, thermal inertia was uniformly assumed to be 150 tiu. In a similar way, we prepared 10 calculated images with constant (uniform) inertia every 50 or 100 tiu from 150 to 800 tiu in order to compared the TIR temperature images. They were compared with the observed data, and the most appropriate thermal inertia was determined for each pixel, resulting in the color map

shown in Fig. 3. Note that there are some area, especially, at the part of edges of boulders and shade boundary, at where the thermal inertia cannot be evaluated due to mismatching of images in pixel level.

Figure 3 shows four interesting features as follows; (1) The red arrows pointing to the shadowed region adjacent to boulders, indicate a thermal inertia of 200-300 tiu, which is almost consistent with that of Ryugu global average. There was no difference in thermal inertia between shadowed areas and newly sunlit areas. (2) The yellow arrows point to the boundary between the boulders and the fine grained surface. It can be seen that the surface of the boulders shows a light blue color (300-400 tiu) while the surface of Ryugu shows a dark blue color (200 tiu). The boulder has slightly higher thermal inertia than that of the fine grained surface. (3) Green arrows indicate localized boulders with high thermal inertia. (4) As indicated by the white arrows, the shaded region next to the largest boulder has slightly higher thermal inertia of 300-500 tiu. At this region, the border line of the shadows are moving from east to west (left to right in the figure), and the shaded area was continued from dawn. This indicate that the skin depth at the shaded area is deeper than at other sunlit areas. It is suggested that the vicinity of the large boulder on this TIR image has higher inertia at deeper part of the surface. As a whole, the thermal inertia at the specific region selected in this study was almost consistent with the global averaged value, however, both of the large boulders and fine grained surface showed wide range of thermal inertia.

Fig. 1 The entire DEM near the second touchdown, created with TIR images. Red is the area used in this analysis.

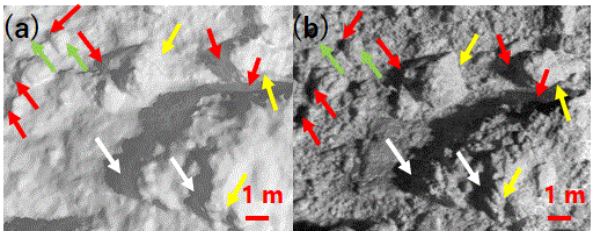

Fig. 2 (a) Results of thermal simulation using a local terrain model. (b) TIR image taken on July 11, 2019 00:47:03 (UTC time).

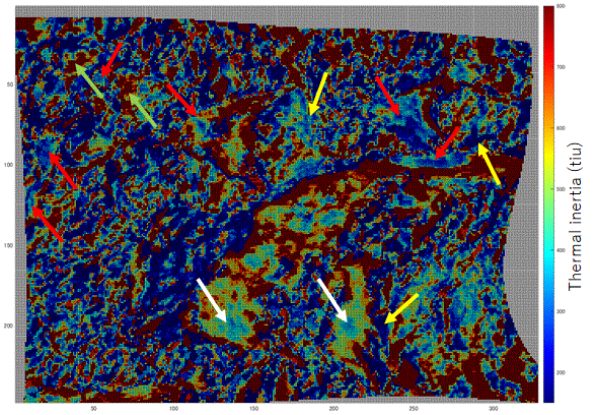

Fig. 3 Color map of thermal inertia corresponding to Fig. 2.

Summary: Using high-resolution TIR images, we were able to produce an accurate local terrain model with a resolution of about 10 cm polygon size. The results of the thermal simulation showed that the thermal inertia of the shadowed region near the boulders and the sunlit area on the surface of Ryugu were almost the same, and the depth dependency could not be observed in many locations. On the other hand, we found some area with high thermal inertia at the shaded area. For example, thermal inertia of the shaded area adjacent to the largest boulder was 300-500 tiu, 200 to 300 tiu higher than that of the averaged thermal inertia. Therefore, there is a difference in thermal inertia in the depth direction at this point.

References: [1] Y. Shimaki. et al. (2020) *Icarus, 348,* 113835. [2] J. Takita. et al. (2017) *Space Science Reviews,208,* 287-315. [3] K. Wada. et al. (2018) *Progress in Earth and Planetary Science,5,* 82. [4] T. Okada. et al. (2020) *Nature, 579,* 518-522.